



HAL
open science

Competition between covalent and non-covalent grafting of fluorescein isothiocyanate on double-walled carbon nanotubes: a quantitative approach

Thomas Lorne, Mónica Jiménez-Ruiz, Stéphane Rols, Jean-Marc Escudier, Juan Rubio-Zuazo, Mohamed Zbiri, Anne-Marie Galibert, Brigitte Soula, Emmanuel Flahaut

► To cite this version:

Thomas Lorne, Mónica Jiménez-Ruiz, Stéphane Rols, Jean-Marc Escudier, Juan Rubio-Zuazo, et al.. Competition between covalent and non-covalent grafting of fluorescein isothiocyanate on double-walled carbon nanotubes: a quantitative approach. *Carbon*, 2017, 123, pp.735-743. 10.1016/j.carbon.2017.07.070 . hal-01813417

HAL Id: hal-01813417

<https://hal.science/hal-01813417>

Submitted on 12 Jun 2018

HAL is a multi-disciplinary open access archive for the deposit and dissemination of scientific research documents, whether they are published or not. The documents may come from teaching and research institutions in France or abroad, or from public or private research centers.

L'archive ouverte pluridisciplinaire **HAL**, est destinée au dépôt et à la diffusion de documents scientifiques de niveau recherche, publiés ou non, émanant des établissements d'enseignement et de recherche français ou étrangers, des laboratoires publics ou privés.



Open Archive TOULOUSE Archive Ouverte (OATAO)

OATAO is an open access repository that collects the work of Toulouse researchers and makes it freely available over the web where possible.

This is an author-deposited version published in : <http://oatao.univ-toulouse.fr/>
Eprints ID : 19344

To link to this article : DOI: 10.1016/j.carbon.2017.07.070
URL : <http://doi.org/10.1016/j.carbon.2017.07.070>

To cite this version : Lorne, Thomas and Jiménez-Ruiz, Mónica and Rols, Stéphane and Escudier, Jean-Marc and Rubio-Zuazo, Juan and Zbiri, Mohamed and Galibert, Anne-Marie and Soula, Brigitte and Flahaut, Emmanuel *Competition between covalent and non-covalent grafting of fluorescein isothiocyanate on double-walled carbon nanotubes: a quantitative approach*. (2017) Carbon, vol. 123. pp. 735-743. ISSN 0008-6223

Any correspondence concerning this service should be sent to the repository administrator: staff-oatao@listes-diff.inp-toulouse.fr

Competition between covalent and non-covalent grafting of fluorescein isothiocyanate on double-walled carbon nanotubes: A quantitative approach

Thomas Lorne^{a, b}, Mónica Jiménez-Ruiz^a, Stéphane Rols^a, Jean-Marc Escudier^c, Juan Rubio-Zuazo^d, Mohamed Zbiri^a, Anne-Marie Galibert^b, Brigitte Soula^b, Emmanuel Flahaut^{b, *}

^a Institut Laue Langevin (ILL), 71 Avenue des Martyrs, BP. 156, F-38042, Grenoble Cedex 9, France

^b CIRIMAT, Université de Toulouse, CNRS, INPT, UPS, UMR CNRS-UPS-INP N5085, Université Toulouse 3 Paul Sabatier, Bât. CIRIMAT, 118, Route de Narbonne, 31062, Toulouse Cedex 9, France

^c Laboratoire de Synthèse et Physico-Chimie de Molécules d'Intérêt Biologique, UMR 5068, Université Paul Sabatier, Bâtiment 2R1, 118, Route de Narbonne, 31062, Toulouse Cedex 09, France

^d European Synchrotron Radiation Facility (ESRF), 71 Avenue des Martyrs, CS 40220, 38043 Grenoble Cedex 9, France

A B S T R A C T

The functionalization of carbon nanotubes with fluorescent molecules is a standard procedure in many toxicity studies aiming at knowing their distribution within cells or whole organisms. Nevertheless, there is a lack of knowledge concerning the efficiency of the grafting processes, and more specifically concerning the question of the competition between covalent and non-covalent grafting. In this work, we investigated the grafting process of the fluorescein isothiocyanate (FITC) onto double-walled carbon nanotubes (DWNTs) using X-ray photoelectron spectroscopy, inelastic neutron scattering spectroscopy and computational simulations. We demonstrated that both covalent and non-covalent grafting occurred during the functionalization with the FITC. Moreover, we showed that a significant fraction of the fluorophore remained simply adsorbed onto the DWNTs despite thorough washing steps, which raises concerning questions about the use of this fluorophore in some toxicity studies and its possible ability to mislead their conclusions.

1. Introduction

Because of their outstanding chemical and physical properties, carbon nanotubes (CNTs) have found applications in many fields, from materials science to nanoelectronics [1], and even in nanomedicine, where they have been used to elaborate drug delivery systems for cancer therapy, biosensors or contrast agents for magnetic resonance imaging [2–4]. The direct consequence of these modern applications is a growing interest in such nanomaterials and the increase in their large scale production [5], leading to an increasing risk of environmental and human exposure. It becomes therefore more and more relevant to evaluate their potential impact on the health and the environment, and the

toxicity studies on this topic are multiplying over the past decade [6–12]. For those toxicity studies it is often required to know the exact location of the CNTs accumulating inside organisms or inside cells. A very common way to track them in such conditions is to functionalize the CNTs with fluorescent molecules which would be illuminated afterwards under a light with appropriate excitation wavelength. Despite the fact that these fluorescence strategies are very cheap and easy to operate, they suffer from a major drawback: they assume that the fluorescent molecule would be permanently linked to the CNTs. It is reasonable to question this assumption as the fluorescent molecules are usually constituted by one or more 6-carbon rings which can strongly interact with the delocalized electron cloud of the CNTs. These non-covalent bonds could later lead to the desorption of the fluorophore once the CNTs reach the complex chemical environment of a living cell and even before entering the cell. Therefore, the fluorescence data could lead to wrong information about the CNTs location. The consequence is

* Corresponding author.

E-mail address: flahaut@chimie.ups-tlse.fr (E. Flahaut).

that a number of published results may be questioned in terms of the actual distribution of the CNTs within cells or at the whole organism level (biodistribution), and the kinetics of this distribution. This may have very important consequences regarding the conclusions about their fate (accumulation, excretion) and thus their toxicity in general. It is thus fundamental to understand the grafting mechanisms and estimate the efficiency of the covalent functionalization of the CNTs as well as the amount of simply adsorbed fluorophores. In order to answer these questions, we chose to study the functionalization of double-walled carbon nanotubes (DWNTs) with a very common fluorophore, fluorescein isothiocyanate (FITC). We used a three step functionalization process to graft the FITC on oxidized DWNTs [13–17]. This work presents a qualitative and quantitative evaluation of the way the fluorophore is bonded to the DWNTs, using two different spectroscopic techniques. First, we performed X-ray photoelectron spectroscopy (XPS) which allowed to probe the surface of the samples and to understand the different types of interactions between the FITC and the DWNTs. Then we characterized the bulk of our samples with the help of inelastic neutron scattering (INS) techniques. Indeed, neutron techniques are especially sensitive to the hydrogen atoms while they have a low sensitivity to the carbon ones. This property makes them a perfect probe of our samples, allowing to highlight the organic molecules since the information on the contribution of CNTs is much reduced. In addition to neutron techniques we used computational techniques such as density functional theory (DFT) calculations (lattice dynamics) in order to gain a better understanding of our samples, provide hypothesis to strengthen data analysis and to be able to derive quantitative information from our experimental results. Based on XPS and neutron techniques, we bring here some evidences that, in the case of the targeted covalent grafting of FITC (one of the most commonly used fluorophore in this kind of research) on CNTs, an important part of the fluorescent molecule is only adsorbed on the nanoparticles despite thorough washing steps, and is thus likely to desorb at some point along its journey within a cell or an organism, potentially leading to wrong conclusions in terms of toxicity.

2. Sample preparation and experimental details

2.1. Sample preparation

DWNTs were synthesized at 1000 °C by catalytic chemical vapor deposition (CCVD) of a mixture of CH₄ (18 mol.%) and H₂ on a Co:Mo: MgO-based catalyst with the elemental composition Mg_{0.99}Co_{0.0075}MO_{0.0025}O. The complete procedure of synthesis of DWNTs was detailed earlier [18,19]. The inner and outer diameters ranged from 0.5 to 2.5 nm and from 1.2 to 3.2 nm, respectively. The median inner diameter was 1.3 nm and the median outer diameter was 2.0 nm. After the CCVD, the obtained composite powder was treated with an aqueous HCl solution, which is an established method for the removal of the oxides and of non-protected residual catalyst nanoparticles without degrading CNTs. The samples were filtered (cellulose nitrate, pore size: 0.45 μm) and washed with deionized water until neutrality. In order to purify the CNTs and remove the remaining metallic impurities and the disorganized carbon, the samples were then treated with a double-step oxidation process widely studied by Bortolamiol and al. [20]. The first step was a 24 h oxidation treatment with HNO₃ (3 M) and the second step was a 5 h treatment using a HNO₃ 65%/H₂SO₄ 95% (1:3) mixture. The double oxidation process was followed by a washing with a NaOH (4 M) solution in order to clean the sample from the remaining carboxylated carbon fragments (CCFs) produced by the oxidation treatments. The purified DWNTs samples so obtained have a very high purity and contains oxygenated functional groups

at their surface (mainly carboxylic) [21–23] which were used as anchor points for the functionalization of the DWNTs. The functionalization of the samples started with the grafting of a 1,4-diaminobutane used as a linker between the DWNTs and the fluorescent molecules. First the carboxylic groups were activated in an oxalyl chloride solution for 24 h at 60 °C (reflux conditions). Then the oxalyl chloride was eliminated and the DWNTs were placed in a solution of tetrahydrofuran (THF) containing the linker (1,4-diaminobutane) and a non-nucleophilic base (N,N-diisopropylethylamine (DIEA)) during 96 h at 30 °C under steering. This first step was common to both samples. After the grafting of the linker part of the sample was simply filtered, washed with THF and freeze-dried, constituting the sample named “DWNT-diamine”. The rest of the material was filtered, washed and kept in THF. The DIEA was added to the suspension of DWNTs in the THF. Finally, a solution of FITC dissolved in THF was added and the resulting suspension was sealed with parafilm and kept away from light for 72 h under stirring at room temperature. Finally the suspension was filtered, the functionalized DWNTs were washed with THF and freeze-dried. This constituted the sample named “DWNT-diamine-FITC”, corresponding to fluorescent DWNTs (see [supporting information for the complete detailed procedure](#)).

2.2. X-ray photoelectron spectroscopy (XPS)

XPS measurements were performed using a standard ultrahigh vacuum (UHV) chamber with a base pressure of 1×10^{-10} mbar equipped with a hemispherical analyzer and a non-monochromatic dual Mg/Al x-ray source. For the present measurements the Mg anode was used providing X-ray photons with energy of 1253.6 eV. As the sample are powders, we used copper adhesive tape to stick them to the sample holder which is made of molybdenum. Both the adhesive and the sample holder are conductive materials allowing the charges to be evacuated. Samples were pumped down overnight within the XPS load lock chamber (1×10^{-8} mbar) prior to introduction into the analysis chamber.

2.3. Inelastic neutron scattering

The INS experiments were performed using a filter-analyzer neutron spectroscopy technique on IN1-LAGRANGE spectrometer at the Institut Laue-Langevin (Grenoble, France).

IN1-LAGRANGE (LArge GRaphite ANalyser for Genuine Excitations) is an indirect geometry spectrometer based on the space focusing of neutron scattered by the sample (cooled at 5 K) in a very large solid angle, which are all recorded with a relatively small single counter. It owns a cooled Be-filter combined with a large area pyrolytic graphite (PG) crystal analyzer that collects the scattered neutrons and define their final energy to 4.5 meV. As the final energy is fixed, the incident neutron beam energy reaching the sample is tunable. Indeed, IN1-LAGRANGE uses a set of double focusing neutron monochromators allowing the incident neutron energy, provided by the hot neutron source of the ILL, to be scanned over a wide range of 4–600 meV. The experiments were performed using the Cu331 monochromator. With such configuration the incident energy (E_i) was scanned from 62 meV up to 500 meV and the energy resolution was around 1.5–2% of E_i. The measured intensity is directly proportional to the generalized phonon density of states (GDOS_{exp}), which allows a direct comparison with the calculated neutron spectra [24,25]. The samples were heated up to 380 K under vacuum (10^{-6} bar) in order to remove the water trapped within the DWNTs samples and sealed inside standard aluminium cylindrical containers with an indium O-ring.

2.4. DFT calculations of the vibrational density of states

The simulations were performed using the software Materials Studio [34]. The calculations of the normal modes associated to our samples were performed considering three model systems. For each model the DWNT have been replaced by a periodic single-walled carbon nanotube (SWNT) (6,6) of 8.14 Å diameter placed in a triclinic lattice, in order to decrease the number of atoms and optimize the computational time. The SWNT was oriented parallel to the c vector of the lattice and the lattices parameters were chosen as following: $a = 15.000\text{--}20.000$ Å, $b = 20.000$ Å, $c = 14.595$ Å; $\alpha = 90^\circ$, $\beta = 90^\circ$, $\gamma = 120^\circ$. Three models have been chosen to represent the three extreme cases that can be found at the end of the grafting process. The first model is a SWNT with one molecule of linker covalently bonded to it, representing the case of 0% of FITC grafted, in the following will be referred as “SWNT-linker” (see Fig. 1-a). The second model is a SWNT that corresponds to the “SWNT-linker” model but where, in addition, one molecule of FITC is covalently bonded to the linker, and represents the case of 100% of fluorophore covalently grafted. It will be referred as “SWNT-linker-Fluo” (see Fig. 1-b). For each of these two models, a search of the lowest energy space conformation was performed using the module “Conformers” in Materials Studio. The rotatable torsion angles of the nitrogen bonds in our models were let free and a systematic search was performed by rotating step by step each of them. The other degrees of freedom (carbon bonds of the organic molecules) were kept constrained since the more stable space conformations of polyamines were found for linear carbon chains [26–28]. At each step a coarse geometry optimization was performed and the total energy of the system was calculated. Then, the lowest energy space

conformation was kept for the density functional theory (DFT) calculations. Finally, the third model is constituted of one SWNT and one FITC weakly bonded through π -stacking interactions, representing the case where 100% of the FITC is non-covalently grafted. It will be referred as “SWNT@Fluo” from now on (see Fig. 1-c). The DFT calculations were performed using the DMol3 module of Materials Studio with the GGA-PBE functional [29] in order to achieve the fine geometry optimization of the systems after which the residual forces were converged close to zero ($\sim 10^{-3}$). To do so, we used an all electron core treatment and a double numerical plus polarization basis set, with a 10^{-5} energy cutoff, a 10^{-6} SCF tolerance and a gamma k-point sampling. Finally, once an equilibrium structure was reached, lattice dynamics calculations were subsequently performed to obtain the phonon frequencies by diagonalization of the dynamical matrix. The $g(\omega)$ is the sum of the individual atomic contribution to the vibrational density of states and is defined by $g(\omega) = \sum g_i(\omega)$. In order to compare with the GDOS_{exp} it was necessary to calculate a theoretical generalized density of states (GDOS_{th}) taking into account the individual atomic contributions weighted by their respective neutron cross section and mass, and defined by $\text{GDOS}_{\text{th}} \propto \sum \frac{\sigma_i}{m_i} g_i(\omega) e^{-2W_i(Q)}$, where σ_i indicate the experimental individual neutron cross section, m_i is the mass and $W_i(Q)$ is the Debye-Waller factor for the atom i . Since the hydrogen cross section is very large compared to the other atoms of our models, the individual contributions of any atoms are negligible compared to those of hydrogen in the case of INS measurements, and the GDOS_{th} can be then approximated such as $\text{GDOS}_{\text{th}} \approx g_{\text{H}}(\omega) e^{-2W_{\text{H}}(Q)}$, where $g_{\text{H}}(\omega)$ is the hydrogen partial density of states. Finally, in order to reproduce at best the GDOS_{exp} measured in INS experiment the multiphonon events ($M(\omega)$) were

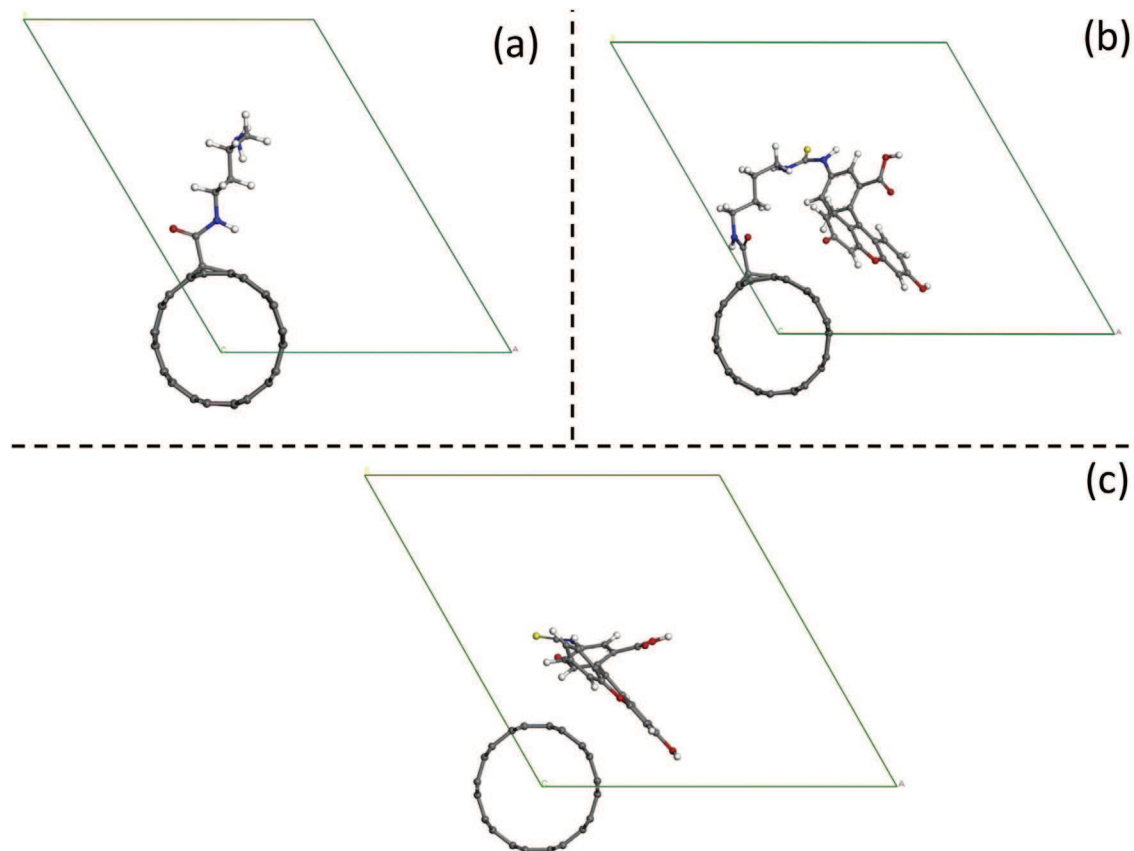


Fig. 1. Representation of the three model systems and their respective lattices, chosen for the DFT calculations. With (a) the SWNT-linker, (b) the SWNT-linker-Fluo and (c) the SWNT@Fluo. (A colour version of this figure can be viewed online.)

taken into account. Indeed, as IN1-LAGRANGE is an indirect geometry spectrometer the momentum transfer (Q) increases with the energy transfer [30], and as the $M(\omega)$ are Q -dependent [31,32], they play an important role in the shape of the measured spectra. The G_{th} is thus defined by $G_{th} \approx g_H(\omega)e^{-2W_H(Q)} + M(\omega)$.

3. Results and discussion

3.1. X-ray photoelectron spectroscopy results

The experimental XPS spectra have been fitted with Voigt functions using a fixed Gaussian width of 0.8 eV corresponding to the overall experimental resolution. For each spectrum the same procedure was followed using the software "UNIFIT". First the satellites and the background were removed. The XPS spectra obtained for each sample were then shifted in energy to compensate charge effects. The C1s orbital main C-C peak was centered at 284.6 eV accordingly to the literature. Then, the appropriate number of components used for fitting the different contributions to each spectrum were chosen according to the number of nitrogen containing chemical groups in the sample. Finally, one sample of pure FITC and the sample "DWNT-diamine" were measured as references and the results so obtained were used to fit the results obtained for the sample "DWNT-diamine-FITC".

For all the spectra, the fit was considered converged when the χ^2 tolerance was reached and was equal to 1.10^{-9} .

3.1.1. FITC

A FITC molecule contains only one type of nitrogen involved in a $-NCS$ chemical group (see inset of Fig. 2-a). The peak position, the area and the Lorentzian full width at half maximum (wL) were let unconstrained during the fitting procedure.

Fig. 2-a shows the result of the XPS measurement of the FITC in the N1s orbital binding energy region (blue marked line) and displays the result of the peak fitting following the procedure mentioned above (green line).

The $-NCS$ group contribution to the N1s peak can be defined by its characteristic position and FWHM, while its area is characteristic of the number of nitrogen atoms involved in such groups. The fitting parameters are listed in Table 1.

Table 1

Fitting parameters of the $-NCS$ groups XPS peak from the FITC sample.

Chemical group	$-NCS$
Peak Position (eV)	400.1 ± 0.0
wL	1.4 ± 0.0
Area	2493.69 ± 0.07

3.1.2. DWNT-diamine

The DWNT-diamine sample has in principle two types of nitrogen atoms: the first type is involved in a $-NH$ group and participates to the chemical bond that links the linker to the nanotube. The second type, located at the other extremity of the linker, is involved in a $-NH_2$ group (see inset of Fig. 2-b). For the fitting procedure, the peaks positions and the wL were let unconstrained, and the area of the two peaks were constrained to be equal.

Fig. 2-b shows the result of the XPS measurement of the DWNT-diamine in the N1s orbital binding energy region (blue marked line) and displays the results of the peak fit of the two chemical groups contributions to the spectrum: $-NH_2$ groups (red line) and $-NH$ groups (blue line) [33].

Now that the $-NH_2$ and the $-NH$ contributions to the N1s peak have been fitted, we can define the position and the wL that are characteristic of the latter group signals. The fitting parameters are listed in Table 2.

3.1.3. DWNT-diamine-FITC

This sample is more complex than the previous ones in terms of species and chemical groups. It is necessary to define the different species that are present in the sample and which contribute to the XPS N1s peak in order to be able to fit correctly the data. For this sample we developed three models (see Fig. 3) corresponding to the three different configurations which could occur at the surface of the DWNTs:

1. The diamine did not react with the FITC and remained unchanged. (Model I)
2. The diamine and the FITC did react together and are covalently bonded. (Model II)

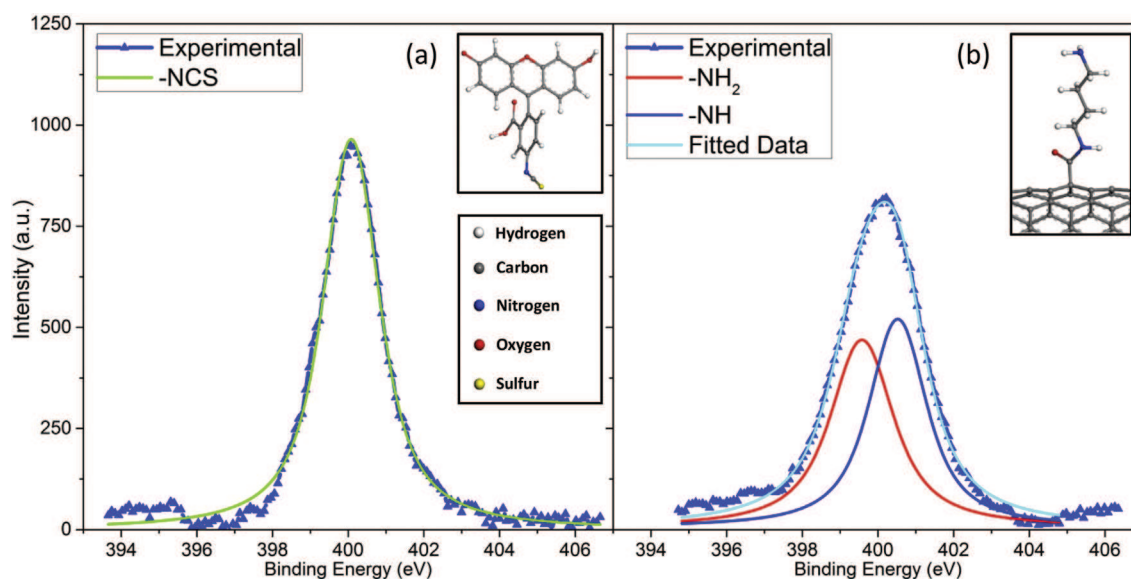


Fig. 2. Experimental results of XPS measurements in the N1s orbital of (a) the FITC and (b) the DWNT-diamine, and respective results of the fitting. (A colour version of this figure can be viewed online.)

Table 2

Fitting parameters of the $-\text{NH}_2$ and $-\text{NH}$ contribution to the N1s peak from the DWNT-Diamine sample.

Chemical group	$-\text{NH}_2$	$-\text{NH}$
Peak Position (eV)	399.6 ± 0.0	400.6 ± 0.0
wL	1.68 ± 0.06	1.45 ± 0.04
Area	1370.67 ± 25.05	1370.67 ± 25.05

3. The FITC did not react with a linker, remained unchanged and has been π -stacked at the surface of the DWNTs. (Model III)

The DWNT-Diamine-FITC sample contains three different types of nitrogen atoms. The first type is involved in $-\text{NH}_2$ groups and is provided by the diamine that stands in the Model I (diamine-I). The second type of nitrogen is involved in $-\text{NCS}$ chemical groups, they are provided by the FITC-III belonging to the Model III presented above. The FITC-III is stacked at the surface of the CNTs and was not able to react with a diamine. Therefore, its $-\text{NCS}$ group remained unchanged. Finally, the last type of nitrogen atom is involved in $-\text{NH}$ groups. They are shared between the diamine-I that did not react with any FITC (Model I) and the diamine-II that did react (Model II). Concerning the diamine-II, that reacted with the FITC-II, it still owns one of this chemical group involved in the covalent bond with the nanotube, but exhibits two additional $-\text{NH}$ groups as the result of the chemical reaction between the original $-\text{NH}_2$ and $-\text{NCS}$ groups respectively.

Fig. 4 shows the result of the XPS measurement of the DWNT-Diamine-FITC in the N1s orbital binding energy region (blue marked line). The peak positions and the wL obtained with the FITC sample ($-\text{NCS}$) and the DWNT-diamine sample ($-\text{NH}_2$ and $-\text{NH}$) were used directly as fitting parameters, while the areas were left unconstrained. The results of the fit are displayed on Fig. 4 for each group contributing to the N1s XPS peak: $-\text{NH}_2$ (red line), $-\text{NCS}$ (green line) and $-\text{NH}$ (blue line).

From the fitted curves of the different group contributions to the N1s peak, we can obtain their respective positions, areas and wL. The fitting parameters are listed in Table 3.

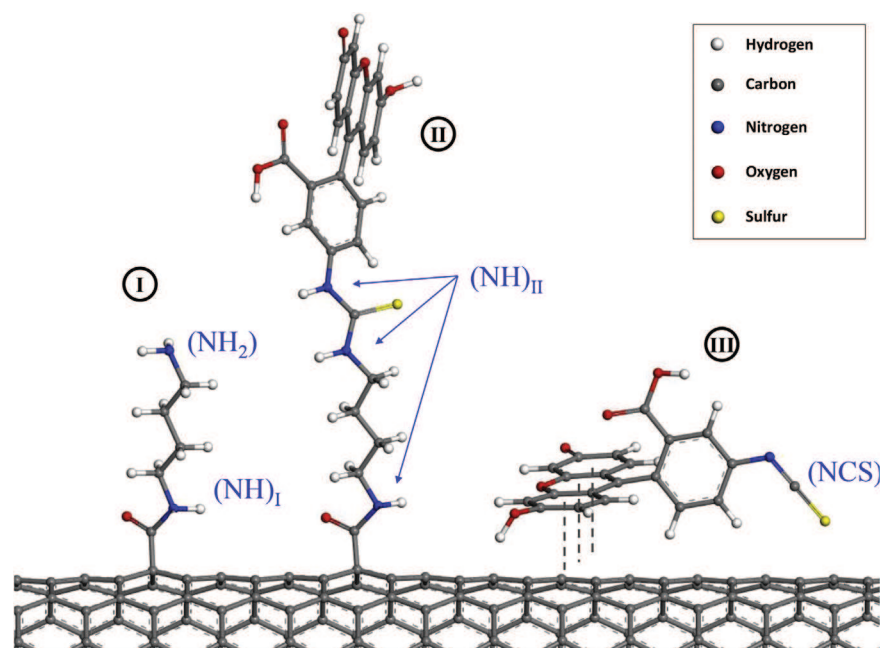


Fig. 3. Illustration of the three models chosen for representing the surface of the DWNT-diamine-FITC sample: (I) SWNT-linker, (II) SWNT-linker-FITC and (III) SWNT@Fluo. (A colour version of this figure can be viewed online.)

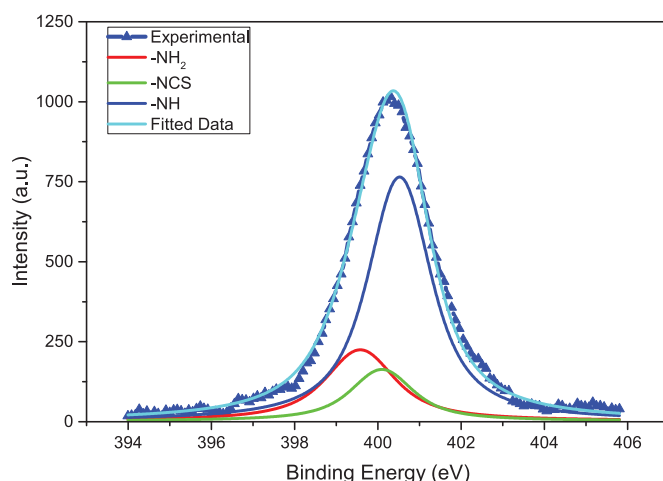


Fig. 4. Experimental results of XPS measurement of the DWNT-diamine-FITC in the N1s orbital binding energy region, and results of the fitting using the reference samples. (A colour version of this figure can be viewed online.)

3.1.4. Process efficiency quantification from the DWNT-diamine-FITC sample

We need to define the relations between the XPS peaks area (that corresponds to chemical groups) and the number of molecules in a given model out of the 3 mentioned above, knowing that the relative proportion of each group in terms of quantities is proportional to its relative proportion of the XPS peak area. Since only the diamine-I contains $-\text{NH}_2$ groups, and there is only one $-\text{NH}_2$ group and only one $-\text{NH}$ group per diamine-I when grafted on a DWNT (see Fig. 3), we can then define $n(\text{diamine-I}) = n(\text{NH})_I = n(\text{NH}_2)_{\text{Tot}} \propto A(\text{NH})_I = A(\text{NH}_2)_{\text{Tot}}$. The amount of diamine-I is now accessible knowing the amount of $-\text{NH}_2$ groups. It is then necessary to define the amount of diamine-II in the sample. Concerning the Model II we find that for 1 mol of diamine-II there are 3 mol of $-\text{NH}$ groups (Fig. 3). We can thus define $n(\text{diamine-II}) \propto \frac{A(\text{NH})_{\text{Tot}} - A(\text{NH}_2)_{\text{Tot}}}{3}$. Finally, we need to define the

Table 3

Characteristics of the different contributions to the N1s peak from the DWNT-Diamine sample.

Chemical group	-NH ₂	-NCS	-NH
Peak Position (eV)	399.6 ± 0.0	400.1 ± 0.0	400.6 ± 0.0
wL	1.68 ± 0.00	1.40 ± 0.00	1.45 ± 0.00
Area	655.18 ± 44.96	415.92 ± 77.67	2023.32 ± 49.25

amount of FITC which did not react with the diamine and, therefore, which is π -stacked onto the DWNTs. As this FITC remained unchanged during the functionalization process, all the Nitrogen atoms have the same signature as the FITC sample, corresponding to -NCS groups. As FITC owns one group per molecule it is then easy to define $n(\text{FITC-III}) = n(\text{NCS})_{\text{Tot}} \propto A(\text{NCS})_{\text{Tot}}$. Finally, using the different areas obtained with the fitting of the DWNT-diamine-FITC sample spectra (see Table 3) the relative proportions of the three models present in the sample were determined and are presented in Table 4 hereafter.

In order to determine the process efficiency we need to define relevant quantities to compare. Here we introduce three different ratios in order to have the clearest vision of what our sample looks like in terms of covalent and non-covalent grafting:

The covalent coverage ratio. It represents the amount of diamine which reacted with the FITC comparatively to the total amount of diamine on the sample before the grafting of the FITC. In that sense it can be interpreted as a measure of the efficiency of the covalent grafting of the fluorophore. It is defined as the ratio between the number of moles of the diamine that reacted with the FITC and the total number of moles of diamine in the sample:

$$R_{cc} = \frac{n(\text{diamine-II})}{n(\text{diamine-I}) + n(\text{diamine-II})} \propto \frac{A(\text{NH})_{\text{Tot}} - A(\text{NH}_2)_{\text{Tot}}}{A(\text{NH})_{\text{Tot}} + 2 \times A(\text{NH}_2)_{\text{Tot}}} \quad (1)$$

The non-covalent grafting ratio. It represents the amount of FITC which is π -stacked onto the carbon nanotubes comparatively to the total amount of FITC in the sample. It gives a measure of the proportion of fluorophore which did not react during the process but which is still present in the sample. It is defined as the ratio between the number of moles of FITC that did not react and the total number of moles of FITC in the sample:

$$R_{ncg} = \frac{n(\text{FITC-III})}{n(\text{FITC-II}) + n(\text{FITC-III})} \propto \frac{3 \times A(\text{NCS})_{\text{Tot}}}{3 \times A(\text{NCS})_{\text{Tot}} + A(\text{NH})_{\text{Tot}} - A(\text{NH}_2)_{\text{Tot}}} \quad (2)$$

The covalent grafting ratio. It represents the amount of FITC which is covalently grafted onto the carbon nanotubes comparatively to the total amount of FITC in the sample. It gives a measure of the proportion of fluorophore which did react with the diamine during the process. It is defined as the ratio between the number of moles of FITC that did react and the total number of moles of FITC in the sample, meaning it is simply the inverse ratio of the non-covalent grafting ratio:

Table 4

Relative proportions of the three models constituting the DWNT-diamine-FITC sample given by the XPS measurements.

	Model I	Model II	Model III
Relative proportions	0.43 ± 0.03	0.30 ± 0.02	0.27 ± 0.04

$$R_{cg} = 1 - R_{ncg} = 1 - \frac{3 \times A(\text{NCS})_{\text{Tot}}}{3 \times A(\text{NCS})_{\text{Tot}} + A(\text{NH})_{\text{Tot}} - A(\text{NH}_2)_{\text{Tot}}} \quad (3)$$

Now the relation between the amount of the different organic molecules in the sample and the chemical groups contributing to the XPS N1s orbital peaks area have been defined, and relevant ratios to understand our sample have been established, we can calculate them in order to get an estimation of the functionalization process efficiency. Using eqs. (1)–(3), and using the XPS peaks area summed up in Table 3 we find that $R_{cc} = 0.41 \pm 0.02$, $R_{ncg} = 0.47 \pm 0.05$ and $R_{cg} = 0.53 \pm 0.05$. The R_{cc} indicates that 41% only of the diamine available reacted with the FITC to form a covalent bond (see Fig. 5), which question the efficiency of the grafting process and leaves a lot of room for improvement. Then, the comparison of the R_{ncg} and the R_{cg} seems to show that about 50% of the total amount of FITC is involved in covalent interaction with the DWNTs while the other half of is simply adsorbed at the surface (see Fig. 6). These latter results are very concerning since they indicates that potentially half of the fluorescence could be attributed to relatively weakly bonded fluorophores molecules.

3.2. DFT calculations results

The DFT calculations performed on the three model systems SWNT-linker, SWNT-linker-Fluo and SWNT@Fluo, which represent three limit cases of the grafting process, allow us to understand the changes expected in our experimental data in terms of active vibrational modes. Indeed, Fig. 7 compares the hydrogen partial density of states ($g_H(\omega)$) obtained via DFT calculations for (a) the SWNT-linker, (b) the SWNT-linker-Fluo and (c) the SWNT@Fluo. We were then able to identify characteristic vibrational bands of our model molecules. For instance, in the bending region, the SWNT-linker and the SWNT-linker-Fluo $g_H(\omega)$ present obvious similarities notably the two broad set of modes at 1270–1380 and 1440–1480 cm^{-1} corresponding to the bending vibrational modes of the -CH groups with no particular distinction between the -CH sp^3 (linker) and the -CH sp^2 (FITC). Similar modes were found at 1140–1220 cm^{-1} for the three models, corresponding to -CH

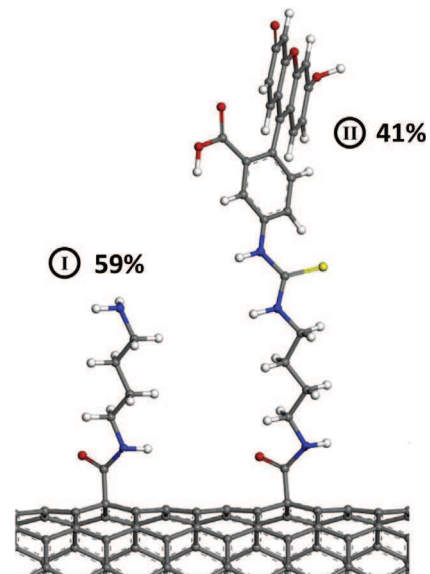


Fig. 5. Representation of the results given by the R_{cc} . (A colour version of this figure can be viewed online.)

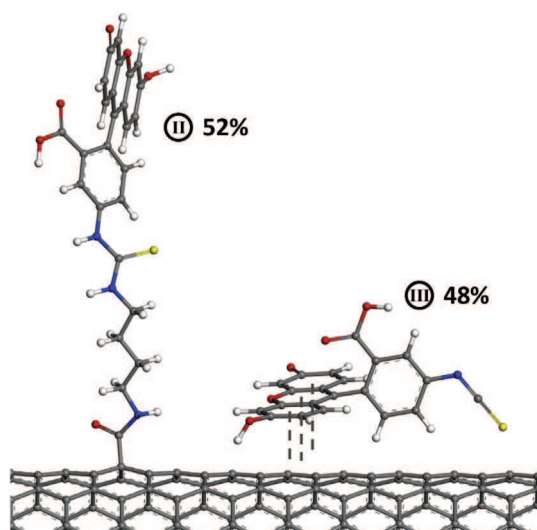


Fig. 6. Representation of the results given by the R_{ncg} and the R_{cg} . (A colour version of this figure can be viewed online.)

bending modes, and, once again, without distinction between the models despite the apparent change in intensity and position. Nevertheless, a major difference is clearly visible between the systems, at 1620 cm^{-1} on Fig. 7-a and disappears completely on Fig. 7-b. This characteristic vibration corresponds to the bending mode of the $-\text{NH}_2$ groups and present the advantage to be isolated from the other modes and to be clearly identifiable. It was naturally chosen as the signature of the disappearance of the $-\text{NH}_2$ groups characteristic of the covalent grafting of the FITC. On the other hand, in the stretching region, signatures of the $-\text{CH sp}^3$ were found on the SWNT-linker and the SWNT-linker-Fluo models between 2890 and 3090 cm^{-1} , and are characteristic vibrational modes of $-\text{CH}$ belonging to the linker. On Fig. 7-b and -c, the presence of the FITC brought new vibrational modes arising at $3100\text{--}3160\text{ cm}^{-1}$ which are characteristic of the $-\text{CH sp}^2$

constituting the fluorescent molecule. Finally, the vibrational modes of the $-\text{NH}$ and $-\text{NH}_2$ and some $-\text{OH}$ groups are located within $3420\text{--}3510\text{ cm}^{-1}$. Unfortunately the vibrational bands are very close to each other, so that we do not expect to see any difference on the GDOS_{exp} in the stretching region if the amount of $-\text{NH}_2$ groups decreases after the grafting process.

3.3. Inelastic neutron scattering results

The measurements performed on IN1-LAGRANGE allowed us to obtain well defined spectra of the DWNT-diamine and the DWNT-diamine-FITC samples, and to have access to several vibrational modes. Fig. 8 shows the experimental generalized density of states (GDOS_{exp}) measured in the energy range $500\text{--}4000\text{ cm}^{-1}$ for the DWNT-diamine (Fig. 8-a) and the DWNT-diamine-FITC (Fig. 8-b) samples (red lines). Fig. 8 also shows the calculated $g_{\text{H}}(\omega)$ of the SWNT-linker model (Fig. 8-a) and the mixing of the $g_{\text{H}}(\omega)$ obtained for the SWNT-linker, the SWNT-linker-Fluo and the SWNT@Fluo models in the proportion of respectively 60%/20%/20% (Fig. 8-b), corresponding to the best fit to the GDOS_{exp} obtained. Both the $g_{\text{H}}(\omega)$ and the mixed $g_{\text{H}}(\omega)$ were convoluted with the experimental resolution (3% of the energy)(cyan lines). Fig. 8 shows as well the corresponding calculated multiphonon contributions for these models (green line) and the resulting theoretical generalized density of states (GDOS_{th}) which corresponds to the sum of the $g_{\text{H}}(\omega)$ and multiphonon contributions, convoluted with the experimental resolution (blue line).

The simulations were based on perfect model systems where the SWNTs were well individualized and all oriented in the same direction. Therefore, the simulation results could not be expected to perfectly fit our data, as can be seen on Fig. 8 in the $500\text{--}1200\text{ cm}^{-1}$ and $2750\text{--}4000\text{ cm}^{-1}$ regions. Indeed, as real samples are much more complex than models, it is not surprising that several vibrational modes could practically be strongly affected by the changes of environment, and appeared to be shifted, broadened or even less intense than the DFT-based predictions. Nevertheless, the simulations performed appeared to fit properly the region of interest comprised between 1200 and 2250 cm^{-1} allowing their use for a

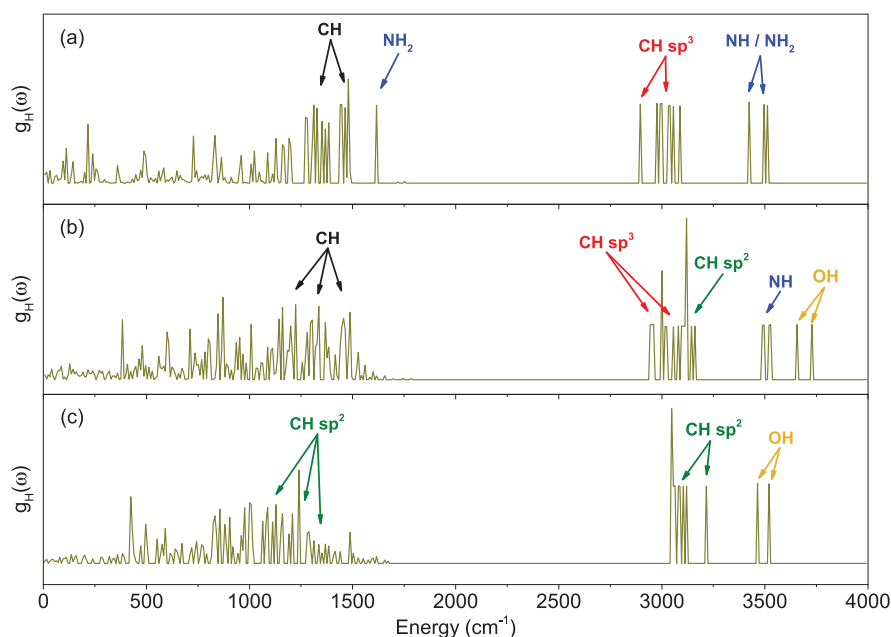


Fig. 7. Comparison of the $g_{\text{H}}(\omega)$ obtained via DFT calculations for the three models: (a) the SWNT-linker, (b) the SWNT-linker-Fluo and (c) the SWNT@Fluo. (A colour version of this figure can be viewed online.)

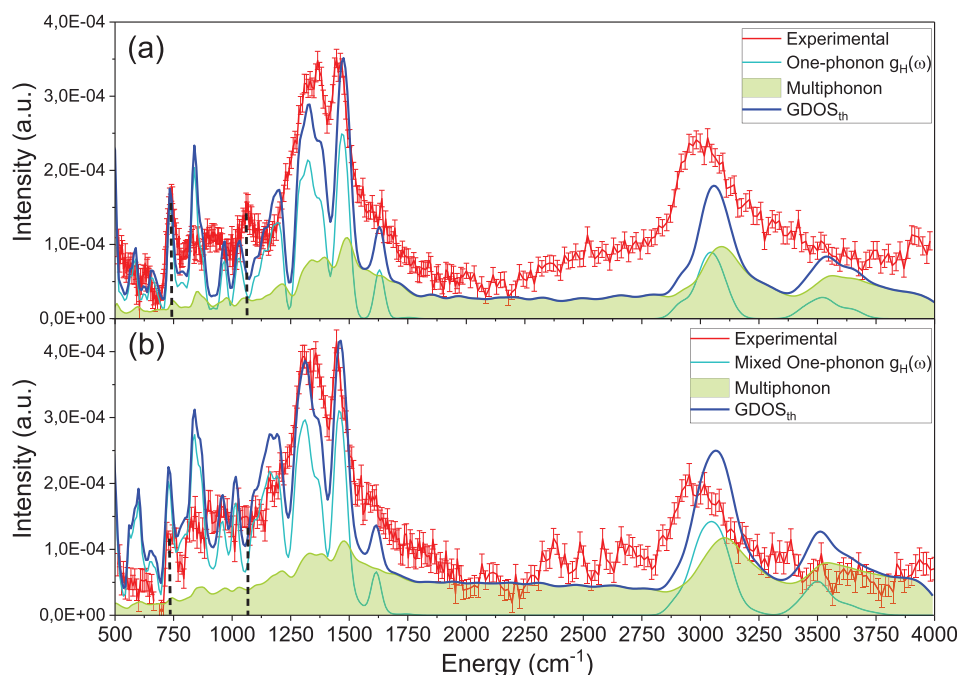


Fig. 8. Comparison of the GDOS_{th} (including the resulting multiphonon contributions) with the INS experimental spectra (or GDOS_{exp}) for (a) the DWNT-diamine and (b) the DWNT-diamine-FITC samples. (A colour version of this figure can be viewed online.)

better understanding of the samples composition.

First of all, clear evidences of the covalent grafting of FITC were found comparing the GDOS_{exp} of the two samples presented in Fig. 8 and the GDOS_{exp} of reference samples (see [supporting information for details](#)). Indeed, the decrease in the vibrational bands located at 740 and 1060 cm^{-1} visible for the DWNT-diamine-FITC sample was associated to the effect of the covalent bonding of the diamine and FITC molecules. Nevertheless, the INS experimental spectra of our two samples are very similar and particularly around 1600 cm^{-1} where we expected to see the largest differences after the grafting process, accordingly to the results provided by the DFT calculations (Fig. 7). Indeed, this vibrational band was supposed to be strongly affected by the number of $-\text{NH}_2$ groups in our samples and should decrease significantly when the FITC reacts with the linker. But, taking into account the multiphonon contributions to the spectra in our simulations we were able to explain this lack of differences in the experimental spectra. Indeed, it is clearly visible on Fig. 8-b that for a mixing ratio of 60%/20%/20% of our three models $g_{\text{H}}(\omega)$, the decrease in intensity undergone by the 1600 cm^{-1} vibration was compensated by the resulting multiphonon intensity associated to the bending region (500–2000 cm^{-1}) fundamental vibrations. By looking at the resulting GDOS_{th} , this vibrational band intensity then appears to be almost unchanged despite the fact that 20% of the linker reacted with the FITC. Various ratios for mixing our three models have been tried and the best fit with the experimental data corresponds to this 60%/20%/20% ratio. These results could indicate that the bulk of the DWNT-diamine-FITC sample is slightly different from its surface (see XPS measurements) which would not be surprising since the DWNTs have a strong tendency to form bundles and that the grafting efficiency could change between the outside and the inside of those bundles. However, some other ratios could still fit reasonably our INS spectrum. Nevertheless, we were able to define that if less than 40% of the SWNT-linker model was taken into account in the mixing ratio, the intensity loss of the 1600 cm^{-1} vibrational mode could not be compensated by the multiphonons

and would have been clearly visible on the DWNT-linker-FITC spectra. Therefore, accordingly to the INS results, we were able to find that in the best covalent grafting case scenario the sample is constituted of 40% of Model I, 30% of Model II and 30% of Model III, which is comparable to the results obtained with the XPS measurements.

4. Conclusion

The quantification of the covalent grafting efficiency of the FITC on DWNTs remains a central question for several toxicity studies. We have shown in this work, based on spectroscopy techniques and calculations, that not only the efficiency of the chemical reaction between the linker and the fluorophore stays below 41%, although we used a grafting protocol very common in the literature, but also that there is a significant amount of fluorophore which remains adsorbed at the surface of the DWNTs after the grafting process, despite the thorough washing procedure. Both, the surface and the bulk of the sample, have been investigated and have shown the same trend. Indeed, the XPS measurements brought information on the surface of the sample and indicated that both covalent and non covalent grafting occurred during the grafting process. It also allowed to make an estimation of the relative proportions of each species at the surface of the sample, and provided concerning results with regards to the amount of FITC simply adsorbed onto the DWNTs. Then, concerning the bulk of the sample, the INS measurement performed on IN1-LAGRANGE coupled with DFT calculations showed strong evidences that the FITC reacted with the diamine. However, the results indicated that the proportions of FITC that reacted with the diamine could be even lower than for the surface but are not contradictory with the estimations provided by the XPS measurements. Finally, these results highlight that, although the amount of fluorescent markers grafted on carbon nanotubes when using a covalent strategy is always considered to be strongly bonded, a non-negligible part may indeed be only adsorbed even after thorough washing of the nanoparticles. This is

likely to lead to a release of the fluorescent marker at some point along the journey of the nanoparticle throughout the cells or the whole organism, and thus to partially wrong conclusions in terms of their fate in terms of biodistribution, accumulation or excretion.

Acknowledgment

The authors would like to acknowledge the grants from the Université Paul Sabatier (UPS) and the Institut Laue-Langevin (ILL) (number ILL-1389.1). We would also like to acknowledge Tifania Bortolamiol for all her work on this topic prior to this project. We would like to acknowledge as well Pierre Lonchambon, Alain Bertoni and Simon Baudoin for the technical support at the chemistry laboratory and on IN1-LAGRANGE. Finally we acknowledge the ILL for the Inelastic Neutron Scattering beamtime allocation and the ILL C-Lab group for the support on simulations.

Appendix A. Supplementary data

Supplementary data related to this article can be found at <http://dx.doi.org/10.1016/j.carbon.2017.07.070>.

References

Full references for this chapter can be found online: <http://dx.doi.org/10.1016/j.carbon.2017.07.070>

- [1] M. Monthieux, P. Serp, E. Flahaut, M. Razafimanana, C. Laurent, A. Peigney, et al., Introduction to carbon nanotubes, in: Springer handbook of Nanotechnology, Springer, 2007, pp. 43–112, http://dx.doi.org/10.1007/978-3-540-29857-1_3.
- [2] F. Lu, L. Gu, M.J. Mezziani, X. Wang, P.G. Luo, L.M. Veca, et al., Advances in bioapplications of carbon nanotubes, *Adv. Mater.* 21 (2) (2009) 139–152, <http://dx.doi.org/10.1002/adma.200801491>.
- [3] Z. Liu, K. Chen, C. Davis, S. Sherlock, Q. Cao, X. Chen, et al., Drug delivery with carbon nanotubes for in vivo cancer treatment, *Cancer Res.* 68 (16) (2008) 6652–6660, <http://cancerres.aacrjournals.org/content/68/16/6652.short>.
- [4] R. Klingeler, S. Hampel, B. Büchner, Carbon nanotube based biomedical agents for heating, temperature sensing and drug delivery, *Int. J. Hyperth.* 24 (6) (2008) 496–505.
- [5] M.F. De Volder, S.H. Tawfick, R.H. Baughman, A.J. Hart, Carbon nanotubes: present and future commercial applications, *Science* 339 (6119) (2013) 535–539, <http://science.sciencemag.org/content/339/6119/535.short>.
- [6] E. Flahaut, M. Durrieu, M. Remy-Zolghadri, R. Bareille, C. Baquey, Investigation of the cytotoxicity of CCVD carbon nanotubes towards human umbilical vein endothelial cells, *Carbon* 44 (6) (2006) 1093–1099, <http://dx.doi.org/10.1016/j.carbon.2005.11.007>, <http://linkinghub.elsevier.com/retrieve/pii/S000862230500672X>.
- [7] M. Bottini, S. Bruckner, K. Nika, N. Bottini, S. Bellucci, A. Magrini, et al., Multi-walled carbon nanotubes induce T lymphocyte apoptosis, *Toxicol. Lett.* 160 (2) (2006) 121–126, <http://dx.doi.org/10.1016/j.toxlet.2005.06.020>, <http://linkinghub.elsevier.com/retrieve/pii/S0378427405001906>.
- [8] J. Cheng, E. Flahaut, S.H. Cheng, Effect of carbon nanotubes on developing zebrafish (*Danio rerio*) embryos, *Environ. Toxicol. Chem.* 26 (4) (2007) 708–716, <http://dx.doi.org/10.1897/06-272R.1/full>.
- [9] C. Salvador-Morales, P. Townsend, E. Flahaut, C. Vénien-Bryan, A. Vlandas, M.L. Green, et al., Binding of pulmonary surfactant proteins to carbon nanotubes; potential for damage to lung immune defense mechanisms, *Carbon* 45 (3) (2007) 607–617, <http://dx.doi.org/10.1016/j.carbon.2006.10.011>, <http://linkinghub.elsevier.com/retrieve/pii/S0008622306005318>.
- [10] F. Mouchet, P. Landois, E. Sarremejean, G. Bernard, P. Puech, E. Pinelli, et al., Characterisation and in vivo ecotoxicity evaluation of double-wall carbon nanotubes in larvae of the amphibian *Xenopus laevis*, *Aquat. Toxicol.* 87 (2) (2008) 127–137, <http://dx.doi.org/10.1016/j.aquatox.2008.01.011>, <http://linkinghub.elsevier.com/retrieve/pii/S0166445X08000295>.
- [11] D. Crouzier, S. Follet, E. Gentilhomme, E. Flahaut, R. Arnaud, V. Dabouis, et al., Carbon nanotubes induce inflammation but decrease the production of reactive oxygen species in lung, *Toxicology* 272 (1–3) (2010) 39–45, <http://dx.doi.org/10.1016/j.tox.2010.04.001>, <http://linkinghub.elsevier.com/retrieve/pii/S0300483X10001745>.
- [12] R. Saria, F. Mouchet, A. Perrault, E. Flahaut, C. Laplanche, J.C. Boutonnet, et al., Short term exposure to multi-walled carbon nanotubes induce oxidative stress and DNA damage in *Xenopus laevis* tadpoles, *Ecotoxicol. Environ. Saf.* 107 (2014) 22–29, <http://dx.doi.org/10.1016/j.ecoenv.2014.05.010>, <http://linkinghub.elsevier.com/retrieve/pii/S014765131400219X>.
- [13] T. Bortolamiol, Nanotubes de carbone biparois : fonctionnalisation et détection in vitro, Ph.D. thesis, Université Paul Sabatier, 2015.
- [14] H. Goto, H.Q. Zhang, E. Yamashita, Chiral stimuli-responsive gels: helicity induction in poly(phenylacetylene) gels bearing a carboxyl group with chiral amines, *J. Am. Chem. Soc.* 125 (9) (2003) 2516–2523, <http://dx.doi.org/10.1021/ja029036c>.
- [15] X. Zhao, M.X. Jia, X.K. Jiang, L.Z. Wu, Z.T. Li, G.J. Chen, Zipper-featured δ -peptide foldamers driven by donor-acceptor interaction. Design, synthesis, and characterization, *J. Org. Chem.* 69 (2) (2004) 270–279, <http://dx.doi.org/10.1021/jo035149i>.
- [16] P. Singh, C. Samorì, F.M. Toma, C. Bussy, A. Nunes, K.T. Al-Jamal, et al., Polyamine functionalized carbon nanotubes: synthesis, characterization, cytotoxicity and siRNA binding, *J. Mater. Chem.* 21 (13) (2011) 4850, <http://dx.doi.org/10.1039/c0jm04064a>, <http://xlink.rsc.org/?DOI=c0jm04064a>.
- [17] E. Harlow, D. Lane, et al., *Laboratory Manual*, Cold Spring Harbor Laboratory, New York, 1988, p. 579, <http://genesdev.cshlp.org/content/2/4/local/back-matter.pdf>.
- [18] E. Flahaut, R. Bacsá, A. Peigney, C. Laurent, Gram-scale CCVD synthesis of double-walled carbon nanotubes, *Chem. Commun.* 12 (2003) 1442, <http://dx.doi.org/10.1039/b301514a>, <http://xlink.rsc.org/?DOI=b301514a>.
- [19] E. Flahaut, A. Peigney, W.S. Bacsá, R.R. Bacsá, C. Laurent, CCVD synthesis of carbon nanotubes from (Mg,Co,Mo)O catalysts: influence of the proportions of cobalt and molybdenum, *J. Mater. Chem.* 14 (4) (2004) 646, <http://dx.doi.org/10.1039/b312367g>, <http://xlink.rsc.org/?DOI=b312367g>.
- [20] T. Bortolamiol, P. Lukanov, A.M. Galibert, B. Soula, P. Lonchambon, L. Datas, et al., Double-walled carbon nanotubes: quantitative purification assessment, balance between purification and degradation and solution filling as an evidence of opening, *Carbon* 78 (2014) 79–90, <http://dx.doi.org/10.1016/j.carbon.2014.06.051>, <http://linkinghub.elsevier.com/retrieve/pii/S0008622314005971>.
- [21] H. Kuzmany, A. Kukovec, F. Simon, M. Holzweber, C. Kramberger, T. Pichler, Functionalization of carbon nanotubes, *Synth. Met.* 141 (1–2) (2004) 113–122, <http://dx.doi.org/10.1016/j.synthmet.2003.08.018>, <http://linkinghub.elsevier.com/retrieve/pii/S0379677903005319>.
- [22] H. Yu, Y. Jin, F. Peng, H. Wang, J. Yang, Kinetically controlled side-wall functionalization of carbon nanotubes by nitric acid oxidation, *J. Phys. Chem. C* 112 (17) (2008) 6758–6763, <http://dx.doi.org/10.1021/jp711975a>.
- [23] K.A. Worsley, I. Kalinina, E. Bekyarova, R.C. Haddon, Functionalization and dissolution of nitric acid treated single-walled carbon nanotubes, *J. Am. Chem. Soc.* 131 (50) (2009) 18153–18158, <http://dx.doi.org/10.1021/ja906267g>.
- [24] Lorne, T., Flahaut, E., Jimenez-Ruiz, M., Rols, S., [dataset] Understanding the Grafting of Fluorescent Molecules on Double-walled Carbon Nanotubes, Institut Laue-Langevin (ILL) doi:10.5291/ILL-DATA.7-05-432. 2015. URL doi:10.5291/ILL-DATA.7-05-432.
- [25] T. Lorne, E. Flahaut, M. Jimenez-Ruiz, S. Rols, Understanding the Grafting of Fluorescent Molecules on Double-walled Carbon Nanotubes, Institut Laue-Langevin (ILL), 2016, <http://dx.doi.org/10.5291/ILL-DATA.7-05-461>.
- [26] E. Agostinelli, M.P.M. Marques, R. Calheiros, F.P.S.C. Gil, G. Tempera, N. Viceconte, et al., Polyamines: fundamental characters in chemistry and biology, *Amino Acids* 38 (2) (2010) 393–403, <http://dx.doi.org/10.1007/s00726-009-0396-7>.
- [27] M.P.M. Marques, L.A.E. Batistadecarvalho, Vibrational spectroscopy studies on linear polyamines, *Biochem. Soc. Trans.* 35 (2) (2007) 374–380.
- [28] First general workshop, [held in torremolinós, near Málaga from 5–8 november 1998]. No. COST 917/european commission, directorate-general science, research and development, in: D.M.L. Morgan, Europäische Kommission (Eds.), *Biogenically Active Amines in Food*; Luxembourg: off. For off. Publ. of the European Communities, vol. 4, 2000. ISBN 978-92-828-8730-1.
- [29] J.P. Perdew, K. Burke, M. Erzerhof, Generalized gradient approximation made simple, *Phys. Rev. Lett.* 77 (18) (1996).
- [30] A. Ivanov, M. Jimenez-Ruiz, J. Kulda, IN1-LAGRANGE – the new ILL instrument to explore vibration dynamics of complex materials, *J. Phys. Conf. Ser.* 554 (2014) 012001, <http://dx.doi.org/10.1088/1742-6596/554/1/012001>, <http://stacks.iop.org/1742-6596/554/i=1/a=012001?key=crossref.f7569efc02188f75984610a03cad54d>.
- [31] J. Dawidowski, F.J. Bermejo, J.R. Granada, Efficient procedure for the evaluation of multiple scattering and multiphonon corrections in inelastic neutron-scattering experiments, *Phys. Rev. B* 58 (2) (1998) 706, <http://dx.doi.org/10.1103/PhysRevB.58.706>.
- [32] J. Dawidowski, G.J. Cuello, M.M. Koza, J.J. Blostein, G. Aurelio, A.F. Guillermet, et al., Analysis of multiple scattering and multiphonon contributions in inelastic neutron scattering experiments, *Nucl. Instrum. Methods Phys. Res. Sect. B Beam Interact. Mater. Atoms* 195 (3) (2002) 389–399, <http://www.sciencedirect.com/science/article/pii/S0168583X02011333>.
- [33] C. Wagner, A. Naumkin, A. Kraut-Vass, J. Allison, C. Powell, J. Rumble Jr., NIST Standard Reference Database 20, Version 4.1, 2012. <https://srdata.nist.gov/xps/>.
- [34] BIOVIA Materials Studio, Dassault Systèmes, 2016. <http://accelrys.com/products/materials-studio/>.